An Analog Neural Network Solution to the Inverse Problem of "Early Taction"

Y. C. Pati, P. S. Krishnaprasad, *Fellow, IEEE,* and Martin C. Peckerar, *Senior Member, IEEE*

Abstract—**In this paper we examine an application of analog neural networks to low-level processing of tactile sensory data. In analogy to the term early vision, we call the first level of processing required in tactile sensing early taction. Associated with almost all existing realizations of tactile sensors are fundamental inverse problems that must be solved. Solutions to these inverse problems are computationally demanding. Among such inverse problems, is the problem of "deblurring" or deconvolution of data provided by an array of tactile sensors that is also assumed to be corrupted by noise. We note that this inverse problem is ill posed and that the technique of regularization may be used to obtain solutions. The theory of nonlinear electrical networks is utilized to describe energy functions for a class of nonlinear networks and to show that the equilibrium states of the proposed network correspond to regularized solutions of the deblurring problem. An entropy regularizer is incorporated into the energy function of the network for the recovery of normal stress distributions. It is demonstrated by means of both computer simulations and hardware prototypes that analog neural networks provide an elegant solution to the need for fast, local computation in tactile sensing. An integrated circuit prototype of the proposed network that has been designed and fabricated is discussed as well.**

I. Introduction

RECENT years have seen a significant increase in the complexity of tasks performed by robotic manipulators. As the complexity of these tasks continues to grow, the need for automated tactile sensing becomes increasingly evident. The term tactile sensing, as used here, refers to the continuous sensing of forces over regions of contact. Included in this definition of tactile sensing are the more rudimentary operations of binary contact sensing and pressure sensing.

Since the specific requirements of robot tactile sensing have not as yet been clearly defined, it is often useful to view tactile sensing in humans as a model for artificial tactile sensing. Tactile sensing in humans is a dynamic process in which dexterous hands are used in conjunction with dense arrays of subcutaneous sensors to extract information about the contact that is necessary for feature identification and formulation of manipulation strategies (see [1]). An "ideal" artificial tactile sensing system should strive to perform a similar function.

The problem of tactile sensing can be hierarchically separated into three stages.

At the lowest level of the hierarchy, there are the device level problems of designing a tactile sensory device and of designing a dextrous manipulator to be equipped with such sensors. It has been suggested [2], [53] that tactile sensors should be distributed in arrays on thin, flexible, compliant substrates. Also, since tactile sensing is based upon physical contact, it is required that the entire structure comprising the tactile sensors be mechanically durable and robust against environmental variations.

Given data from the tactile sensors, the second stage of the hierarchy is concerned with low-level processing and extraction of information. For example, often raw data provided by the sensors are not measurements of contact forces but are related in some manner to the stress profile over the region of contact. In such instances, the inverse problem of determining the stress at the contact surfaces must be solved in order to obtain a meaningful interpretation of the sensory data. Detection of edges, extraction of geometric information, and identification of conditions such as slippage are further examples of tasks to be performed at this level of the hierarchy. It is this level of tactile sensory data processing that we term *early taction*.

The top-most level in this hierarchical picture of tactile sensing is the level at which decisions are made, based upon information provided by the two previous stages. Formulation of manipulation strategies is performed at this level. For example, if a condition of slippage has been recognized, a manipulation strategy should be formulated so as to alleviate this condition. Also at this level of processing, decisions are made regarding the identification of a grasped object based upon information about texture, shape (which could have been determined from knowledge of edges), and material (which may possibly be determined from thermal conductivity).

It is among the goals of this paper to take a step toward integrating the two lowest levels of this hierarchy.

Several aspects of tactile sensing are of a very similar nature as problems encountered in computational vision. Essential differences lie in the fact that, unlike vision sensors, which are remotely located with respect to their target, tactile sensors are required to be in physical contact with their targets. The "deblurring" problem considered in this paper is an example

Manuscript received September 11, 1989; revised February 1, 1991. This work was supported in part by the National Science Foundation's Engineering Research Centers Program under Grant NSFD CDR 8803012, by the Air Force Office of Scientific Research under Contract AFOSR-88-0204, and by the Naval Research Laboratory. Portions of this work were presented at the IEEE Robotics and Automation Conference, Philadelphia, PA, April 24–29, 1988.

Y. C. Pati is with the Systems Research Center and the Electrical Engineering Department, Univeristy of Maryland, College Park, MD 20742, and the Nanoelectronics Processing Facility, Code 6804, U.S. Naval Research Laboratories, Washington, DC 20375.

P. S. Krishnaprasad is with the Systems Research Center and Electrical Engineering Department, University of Maryland, College Park, MD 20742.

M. C. Peckerar is with the Nanoelectronics Processing Facility, Code 6804, U.S. Naval Research Laboratories, Washington, DC 20375 and the Electrical Engineering Department, University of Maryland, College Park, MD 20742.

IEEE Log Number 9105403.

of a problem that also arises in computational vision. Edge detection, which used in vision to determine boundaries within the visual field, is required in tactile sensing to identify physical edges of objects and locate holes to determine shape. A similar analogy can be drawn between motion detection in vision and identifying slippage in tactile sensing.

The set of processes that recover physical attributes of visible three-dimensional objects from two-dimensional visual (intensity) images is collectively termed *early vision*. In a similar manner, the elements of the second hierarchical level of tactile sensing may be collectively termed *early taction*. Early taction then can be defined as the set of processes that recover the three-dimensional attributes of an object and properties of the established contact from two-dimensional arrays of sensor measurements. As yet, the set of problems of which early taction is comprised have not been clearly defined, but recovery of stress over the contact region, edge detection, and identification of slippage are likely among them. As in vision, there is a need in tactile sensing to identify and formalize the problems involved and then devise sensible solutions to these problems.

The methods of this paper are essentially motivated by the requirements of *fast* and *local* processing of tactile sensory data. In humans, useful information is often acquired through active manipulation. A grasped object is often scraped, rolled, and mutilated to determine its shape and other properties [2], [53]. Therefore, it is reasonable to assume that in robots, as in humans, static contact analysis together with dynamic analysis will prove to be useful. *This dynamical aspect of tactile sensing, together with the fact that tactile sensing is generally to be applied in a "real time" environment, implies the need for fast processing of tactile sensory data.* Signals derived from tactile sensors are often measurements of minute force-induced deviations in physical or electrical characteristics of materials. Processing of the signals at this stage is primarily comprised of a number of ill-posed problems that are highly sensitive to noise. Transmission of these (already "weak") signals to remote locations for processing would invariably result in substantial further corruption of the signal and thereby diminish the integrity of the results of any processing. Local processing of tactile sensory data can be further justified on the basis of the desirability of distribution of processing tasks in a robot and compression of data to be transmitted to the CPU. For recent work focusing on implementation of such local processors in analog VLSI in various sensory processing contexts, see [3].

In this paper we discuss a framework within which at least some of the second level of tactile information processing may be performed. The approach taken is designed to meet the requirement of local fingertip processing as well as the demand for fast computation. The problem considered here is the determination of stress due to contact at the boundary of an elastic medium given (noise-corrupted) measurements of induced strain within the medium. In order to meet the requirements of fast local fingertip processing, the paradigm of neural networks is considered.

Inspired by the work of neurophysiologists, psychologists and other researchers on the mechanisms of computation, learning, and memory in biological systems, artificial neural networks are an attempt to reproduce the computational efficiency observed in the nervous system. An artificial neural network may be loosely defined as a highly interconnected network of simple processing units. The processing units themselves are rarely more than simple amplifiers (usually nonlinear amplifiers such as those with sigmoidal characteristics are used), yet neural networks have in many instances demonstrated an ability to solve complex problems. The computational power of artificial neural networks is embedded in the nature of connectivities between the processing units (or *neurons*) of which they are composed. Neural networks[1] are usually regarded as being comprised of layers of neurons and the interconnections among them. Associated with a connection (also called a *synapse*) between two neurons, say neuron i and neuron j, is a number w_{ij} called the *weight* of the connection (sometimes referred to as the *synaptic weight*) between neuron i and neuron j, which determines the effect that the output of neuron i has upon the activity of neuron j. For example, if the output of neuron i is v_i, then the input to neuron j due to the connection of neuron i to neuron j is given by $w_{ij}v_i$. It is the connectivity profile (distribution of connection weights) that determines the computational task performed by any given network. The nature of computation in a neural network is both parallel and asynchronous.

The paradigm of neural networks also provides a formalism for the analog hardware implementation of inherently parallel algorithms. Biological neurons are often modeled as integrators (with the sum of all inputs to the neuron as the integrand) composed with output functions. In terms of analog circuits this corresponds to a simple RC integrator circuit followed by an amplifier with the desired characteristics. Connections between neurons can be implemented as resistors ($w_{ij} = 1/R_{ij}$) since Ohm's law dictates that the current input to neuron j due to the output voltage v_i of neuron i is $R_{ij}v_i$. Hence, having arrived at a neural network model for computation, implementation of the network as an analog electrical circuit is a natural extension [3], [44], [50], [52].

Integrated circuit implementation of neural networks to perform some of the tasks of early taction would provide fast computation that can be performed in close physical proximity to the sensors.

In Section II, a particular inverse problem that arises in the context of tactile sensing is introduced. The inverse problem is formulated as a variational principle and "regularization" is used to compensate for the ill posedness of the problem and provide for reliable computation in the presence of sensor noise.

In Section III some aspects of nonlinear RC electrical networks are discussed. It is shown that under certain conditions it is possible to guarantee stability and explicitly determine a strict Lyapunov function for such a network. Since such a Lyapunov function is minimized in the course of natural time evolution of the network, steady-state outputs of the network correspond to the solutions of a minimization problem (defined by the Lyapunov function).

[1]The term *neural networks* will be used in reference to artificial neural networks unless otherwise indicated.

An analog neural network to solve the inverse problem of tactile sensing is described in Section IV. Using the results of Section III, an energy function for the proposed network is determined and shown to be equivalent to the variational principle formulated in Section II for regularized solution of the inverse problem. Computer simulations of the proposed network are presented in order to evaluate performance of the network in the presence of noise. Experimental results from a prototype breadboard model of the network as well as a preliminary attempt at integrated circuit implementation of the network are also discussed.

II. Inverse Problems in Tactile Sensing

In this section, we examine the fundamental inverse problem that arises in the context of robot tactile perception. Inverse problems of a similar nature also arise in the field of computational vision in early vision problems that have often been designated as inverse optics (see Poggio and Koch [4]). Hadamard [5] in 1923 defined a problem to be well-posed if: 1) the solution exists, 2) the solution is unique, and 3) the solution depends continuously on the initial data. If any of the above three criteria are not satisfied, the problem is said to be ill posed. Most inverse problems that arise in physical settings (such as those in early vision) are ill posed in the sense defined by Hadamard and thus require special techniques to solve.

Numerous tactile sensors have been designed and fabricated for use with robotic end-effectors. All such sensors have been based on the deformation of materials by contact forces and the measurement and interpretation of the deformation to determine the forces inducing it. Examples of some approaches to tactile sensor design can to be found in the survey paper by Lee and Nichols [6]. In typical approaches to tactile sensor design, the transduction process is effected by materials such as piezoelectric polymers [7] and crystals, conductive rubber [7], and piezoresistive materials such as silicon [8]. In [9] a tactile sensor is described that is designed to operate based upon changes in optical characteristics of a material at boundaries (total internal reflection). Such an approach has the advantage of very high spatial resolution since it is not necessary to construct arrays of discrete sensors. Another novel approach to tactile sensor design is described in [10] where transduction is based upon variations in magnetic fields which are measured by a VLSI array of Hall-effect sensors. In most approaches to tactile sensing, there arises an inverse problem, namely, given data from the sensors, determine the force profile at the contact region.

A. Tactile Sensors and Compliant Contact

For the purpose of providing a concrete example, we concern ourselves here with a silicon-based piezoresistive triaxial tactile sensor with a compliant layer designed and fabricated at the Naval Research Laboratories in Washington, DC, and described in [8].

The sensor is constructed as a micromachined silicon mesa surrounded by a thin diaphragm in which a number of diffused piezoresistors are placed (see Fig. 1). An array of these sensors is constructed on a single die and then bonded and packaged

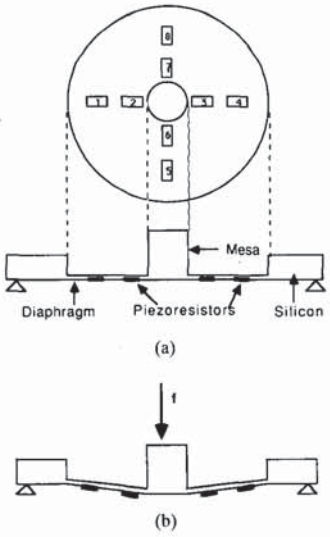

Fig. 1. (a) Schematic top and cross-sectional view of a single piezoresistive tactile sensing element. (b) Application of forces to the mesa deforms the diaphragm, causing changes in the resistance of the piezoresistors.

to be mounted on a robot fingertip. Sensitivity of the tactile sensor is determined by the magnitude of strain induced in the resistors by a given force. In order to increase sensitivity of the sensors, it is necessary to decrease the thickness of the diaphragm and thereby increase the likelihood of its rupture due to excessive force. A layer of compliant material such as rubber or polyimide is used to cover the array of sensors. The use of a compliant layer for fingertip contact serves four beneficial functions.

1) The compliant layer serves to provide damping against large impulsive contact forces, thereby protecting the sensors from damage.
2) In order to facilitate a stable grasp it is desirable to enhance friction at the contact surfaces. For given material at the contact surface, this can be achieved by maximizing contact area. A rigid material in contact with an irregular or bumpy surface contacts the surface at a few discrete points only, whereas a compliant material can conform to the surface and thus maximize contact area. Since the tactile sensing array provides the desired contact surface on the robot finger, it is beneficial to provide compliant contact atop the array of sensors.
3) The third function of the compliant layer is due to the resultant "blurring" of the contact force distribution that causes information about the entire stress distribution to be passed to each individual sensor element. In the absence of such blurring, determination of the applied stress between sample points would not be possible.
4) Compliant contact is beneficial in establishing well posedness of the grasp problem (see [11]).

Referring to Fig. 2(a), we state a fundamental inverse problem.

Inverse Problem: Given samples of a strain distribution, measured by sensors at a given depth beneath the surface of a compliant layer, the inverse problem of tactile sensing refers

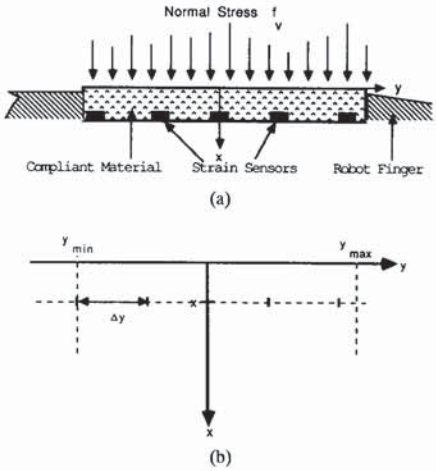

Fig. 2. (a) Stress applied at the boundary of elastic layer with strain sensors beneath surface. (b) Elastic layer extends from $y_{\min}$ to $y_{\max}$ with sensors at depth x beneath the surface at intervals of Δy.

to the problem of determining the surface stress distribution that induced the measured strain.

The inverse problem as stated above is formulated for the particular tactile sensor design we consider here but is similar to the inverse problems associated with many other tactile sensor designs as well.

A. Modeling the Transduction Process

For sake of simplicity in the current discussion, two assumptions are made. 1) The general two-dimensional problem is reduced to a one-dimensional setting, i.e., we consider a linear array of sensors with planar stress applied to the pad. 2) It is also assumed that the compliant layer is actually a homogeneous, isotropic, linear, elastic half-space.

To understand the inverse problem, a model for the forward transduction process is first developed, i.e., a model describing the relationship between stress applied to the compliant layer and the strain induced at a depth x beneath the surface. From the theory of elasticity (see Timoshenko and Goodier [12]), two relationships (for detailed derivations, see [13] and [14]) can be derived. (See also [15].)

Strain at a depth x beneath the surface of the compliant material due to normal stress at the surface is given by

$$p_x(y) = (Kq_v)(y) = \int_{-\infty}^{\infty} k_x^v(y, y_0) q_v(y_0) dy_0 \qquad (1)$$

where $p_x(\cdot)$ is the strain at depth x, $q_v(\cdot)$ is the surface stress, and $k_x^v(\cdot,\cdot)$ is the convolution kernel relating the two given by

$$k_x^v(y, y_0) = \frac{2x((1-\nu)^2x^2 - \nu(\nu+1)(y-y_0)^2)}{\pi E(x^2+(y-y_0)^2)^2} \qquad (2)$$

where ν is Poisson's ratio for the material, E is the modulus of elasticity, and y and y_0 are spatial variables representing location along the surface of the compliant layer. Strain due to tangential stress applied at the surface is given by an analogous formula, with convolution kernel,

$$k_x^t(y, y_0) = \frac{2(y-y_0)((1-\nu)^2x^2 - \nu(\nu+1)(y-y_0)^2)}{\pi E(x^2+(y-y_0)^2)^2}. \qquad (3)$$

Throughout this paper, we only consider the case of normal stress, noting that the case of tangential stress is analogous.[2] Note that these analyticaly derived convolution kernels may not be entirely faithful to the response of an actual array of sensors and that, in practice, the models may have to be empirically determined.

Since measurements of strain are made at a discrete number of points (corresponding to sensor locations), (1) must be discretized. Assume that the sensors are distributed uniformly (equal spacing) beneath the surface of the compliant layer. Let $\Delta_p y$ be the distance between points at which strain is sampled. So, $\Delta_p y = (y_{\max} - y_{\min})/(N-1)$ (see Fig. 2), where N is the total number of sensors. Let $\Delta_q y$ be the distance between points where the stress profile is to be reconstructed. Although it is not necessary for $\Delta_p y$ and $\Delta_q y$ to be equal, for the current discussion we let $\Delta_p y = \Delta_q y = \Delta y$. To obtain a discretized version of (1), let ϵ_x be the vector of strain samples, i.e., $\epsilon_x = (\epsilon_{x_1}, \ldots, \epsilon_{x_N})^T$. Therefore, $\epsilon_{x_i} = p_x(y_{\min} + (i-1)\Delta y)$, $i = 1, \ldots, N$. Similarly, let $f_v = (f_{v_1}, \ldots, f_{v_N})^T$ be the vector obtained from the stress distribution as $f_{v_i} = q_v(y_{\min} + (i-1)\Delta y)$ $i = 1, \ldots, N$. The convolution kernel $k_x^v(\cdot,\cdot)$ can be discretized to form the matrix $T = \{T_{ij}\}$ by letting $T_{ij} = k_x^v(y_i, y_j)$, where $y_i = y_{\min} + (i-1)\Delta y$ for $i = 1, \ldots, N$. Hence, the discretization of (1) results in

$$\epsilon_x = T \cdot f_v. \qquad (4)$$

The discretized inverse problem is precisely the problem of *determining f_v given ϵ_x and T.*

Returning to the third desirable feature of compliant contact, we observe that if we let T be a nonsquare matrix, then in solving the inverse problem we are attempting to reconstruct the surface stress at points along the surface other than those directly above the sensors. This is only possible since the blurring of signals by the compliant layer results in information about most of the stress distribution at the surface being passed to every sensor. The exceptions to this are due to zeros in the convolution kernel.

It can be shown (see Appendix A) that in the infinite dimensional setting of (1), the inverse problem is ill posed. Since the operator K is a compact operator on an infinite dimensional domain, its inverse does not exist as a bounded operator. Hence, Hadamard's third requirement for well posedness is violated. It can also be shown (see Appendix A) that the the manifestation of this ill posedness in the discretized problem (4) is in the ill conditioning of the matrix T. Ill conditioning of the matrix T increases as the discretization is refined. Hence, solutions to the inverse problem in the discrete setting are sensitive to noise in the data.

[2]The analogy referred to here does not extend to the choice of regularizer for the case of tangential stress.

Remark: Extension to the general setting where the sensor array is two dimensional is trivial due to radial symmetry of the convolution kernel. In the one-dimesional case $k_x^v(y, y_0) = k_x^v((y - y_0)^2)$ (see (2)). In the two-dimensional case the convolution kernel $k_{2_z}^v()$ is given by

$$k_{2_z}^v(z, y, z_0, y_0) = k_x^v((z - z_0)^2 + (y - y_0)^2).$$

Discretization in the two-dimensional case leads to a system of equations as in (4) where the vector of measured strains is constructed simply by replacing the double indicies of the entries of the measurement array by a single index. The matrix T in the two-dimensional setting also posseses a Toeplitz symmetric structure.

C. Regularization as a Technique to Solve the Inverse Problem

There exists a large body of literature devoted to approximating the solutions of ill-posed problems (see, e.g., Tikhonov [16] and Tikhonov and Arsenin [17]). One successful technique for solving an ill-posed problem is regularization, which was introduced by Tikhonov [16] in 1963. Ill-posed problems such as the one considered here are often insufficiently constrained and require the imposition of additional constraints for the solution to be well defined. Regularization is a technique in which the problem is formulated as a variational principle that is then used to impose physical constraints on the solution. A variational principle defines the solution to a problem as the minimizer an appropriate cost functional.

Regularization requires the choice of a norm $\|\cdot\|$ and of a stabilizing functional (typically of the form $\|Px\|$). The stabilizing functional embodies the physical constraints of the problem and thus must be chosen only after careful analysis of the physical setting in which the problem arises. Constraints such as smoothness and boundedness of solutions may be imposed by appropriate choice of the stabilizer.

The problem of solving $Kx = y$ can be formulated as a variational principle simply by choosing a norm $\|\cdot\|$ and then finding x that minimizes[3]

$$\|Kx - y\|$$

To regularize the problem additional constraints are imposed through the stabilizing functional.

Standard regularization theory is composed primarily of three methods (see [4] and [18]).

1) Among all x that satisfy the condition $\|Px\| < c$, where c is a constant, find x that minimizes $\|Kx - y\|$.
2) Among all x that satisfy $\|Kx - y\| < \epsilon$, where ϵ is chosen to represent estimated errors, find x that minimizes $\|Px\|$.
3) Find x that minimizes

$$\|Kx - y\|^2 + \lambda\|Px\|^2 \tag{5}$$

where λ is called the *regularization parameter*.

[3] In the case where the solution is unique, this is easily shown to be equivalent to using the generalized inverse $K^\dagger$ to obtain solutions, i.e., letting K^* denote the adjoint of K, $x = (K^*K)^{-1}K^*y = K^\dagger y$ whenever the inverse on the right exsits. If solutions are not unique, $K^\dagger$ picks the solution of minimum norm.

In standard regularization theory, the operator P is linear and the norm $\|\cdot\|$ is derived from an inner product. For such quadratic variational principles, of the form (5), it can be shown that under mild conditions the solution space is convex (which implies the existence, uniqueness, and stability of solutions). In this paper, we will consider other forms of the stabilizing functional that we will denote by $M(x)$. Hence, we will be considering variational principles of the form

$$\|Kx - y\|^2 + \lambda M(x). \tag{6}$$

The regularization parameter λ controls the degree to which a solution is regularized. Small values of λ compromise the degree of regularization in favor of accurately matching the initial data. Very large values of λ may result in very regular but unrealistic solutions.

Regularizing the Tactile Sensing Problem: To regularize the inverse problem of tactile sensing, it is necessary to first identify the generic physical constraints that may be imposed upon the solution. In the case of normal stress applied to the compliant pad (see Fig. 2), it is clear that the unisense nature of the compressive loading on the boundary can be captured by constraining solutions to lie in the positive orthant. To further suppress some of the deleterious effects of sensor noise, the solutions may be constrained to be smooth. Constraining solutions to be smooth may result in inaccurate solutions near physical edges; however, edges may be recovered in a second stage of regularization.

The constraints of nonnegativity and smoothness of the solutions can be embodied in the stabilizing functional by choosing

$$M(x) = \sum_i x_i \log x_i \tag{7}$$

which has the same functional form as Shannon entropy. Hence, in the case of the inverse problem of tactile sensing, the problem is to find a vector $f \in \mathbb{R}^N$ that minimizes

$$\|Tf_v - \epsilon_x\|^2 + \lambda \sum_i f_{v_i} \log f_{v_i} \tag{8}$$

where $T \in \mathbb{R}^{N \times N}$ is a finite matrix approximation to the convolution operator, $\epsilon_x \in \mathbb{R}^N$ is the vector of measured strains, and $f_v \in \mathbb{R}^N$ is the vector of stress components. The norm $\|\cdot\|$ is the standard Euclidean norm on $\mathbb{R}^N$.

The existence and uniqueness of solutions to the minimization problem are easily verified by noting that the positive orthant in $\mathbb{R}^N$ is a convex set and that (8) is a strictly convex function of f_v.

III. Nonlinear Electrical *RC* Networks

Nonlinear electrical networks have been a topic of active research for many years. Hence, there exists a large body of results pertaining to such networks. As elaborated in Section I, the transition from neural networks to electrical networks is not only trivial but natural. Mathematical analysis of neural networks is as yet a developing field. It seems natural to look to the available results for nonlinear electrical networks for insight and understanding of the behavior of neural networks.

Some of the earliest work on electrical networks was done by James Clerk Maxwell in 1873 [19] and is concerned with the distribution of currents and voltages in linear resistive networks. Later work by Tellegen [20], Cherry (1951) [21], and Millar (1951) [22] helped to build a foundation for nonlinear network analysis. In 1964, Brayton and Moser [23] attempted to build a more general theory of nonlinear networks by considering some geometric aspects of such networks. More recently, several researchers have adopted an even more general geometric view of nonlinear networks (see, e.g., [24]–[28]. In these latter works, network dynamics are viewed as flows (differential equations) on nontrivial manifolds (nonlinear spaces). It is clear that a great deal of mathematical machinery has been developed for analysis of nonlinear networks. Applications of the same tools and body of results to neural networks should prove useful.

In this section, one particular application of electrical network analysis to neural networks is demonstrated. We define an energy function for a dynamical system as a functional that is minimized (globally or locally) as a result of the natural time evolution of the system. We present in this section a theorem that is applied in Section IV to determine an energy function for a neural network designed to solve the inverse problem described in Section II.

A. A Theorem on Energy Functions for Nonlinear RC Networks

As in [23], we consider a network composed of branches and nodes with the restriction that a branch connects exactly two nodes. Arbitrarily assigning a direction to the branch currents, we define i_μ as the current flowing from the initial node to the end node of the μth branch in the network. The branch voltage v_μ is defined as the voltage rise measured from the end node to the initial node of the μth branch in the network.

For any network, a complete set of generalized current or voltage coordinates can be chosen. Such a set of variables is complete in the sense that they can be assigned values independently without violation of Kirchoff's laws and that they determine in each branch of the network one of the two variables, branch current or branch voltage. In computing M, the number of defining current coordinates, constant current sources, if any, are not counted as branches and similarly in computing N, the number of defining voltage coordinates, constant voltage sources are not counted as branches. In the particular case of an RC network, a complete set of variables is obtained by considering the voltages across all independent capacitive branches. Two capacitors in parallel are considered as a single capacitive branch with capacitance equal to the parallel combination of the two. We will denote the complete set of variables for an RC network by $v^* = (v_1, \ldots, v_N)$.

The following theorem (which appears in [29]) identifies an energy function for a class of nonlinear RC networks. For the proof of this theorem, see Appendix B.

Theorem 1: Consider a (possibly nonlinear) RC electrical network for which the following hypotheses hold.

H1: The voltages across independent capacitive branches, $v^* = (v_1, \ldots, v_N)$ form a complete set of variables for the network.

H2: Let $i_1, \ldots, i_N$ be the currents through the corresponding capacitive branches (with the appropriate reduction of parallel capacitors) satisfying

$$\frac{\partial i_k}{\partial v_j} = \frac{\partial i_j}{\partial v_k} \qquad j, k = 1, \ldots, N \quad j \neq k$$

Then

1) The equilibrium states of the network correspond to the stationary points of the energy function
$$P(v^*) = -\sum_{j=1}^{N} \int_0^{v_j} i_j dv_j.$$
2) Stable equilibrium states of the network correspond to local minima of $P(v^*)$.
3) If in addition to this $P(v^*) \to \infty$ as $\|v^*\| \to \infty$, then the network is asymptotically stable, i.e., v^* will approach one of the stable equilibrium states of the network (given by the local minima of $P(v^*)$) as $t \to \infty$. ■

As a corollary to the preceding theorem, we consider the case where we would like to formulate the energy function in terms of an auxillary set of independent variables. For proof of the corollary, see [29].

Corollary 1: Assume H1 and H2 of Theorem 1 hold. Let $u^* = (u_1, \ldots, u_N)$ be the auxillary set of independent variables in which we are interested and let $u_i = g_i(v_i), i = 1, \ldots, N$, where $g_i : \mathbb{R} \to \mathbb{R}$. Then if $g_i(\cdot)$, $i = 1, \ldots, N$ are monotone increasing functions, then the conclusions of Theorem 1 hold, and the energy function $P(\cdot)$ may be expressed in terms of the variables u^* by simply replacing each v_i by $g_i^{-1}(u_i)$.

IV. An Analog Neural Network Solution to the Inverse Problem

In this section, an analog neural network is described that has been structured so as to solve the regularized inverse problem of tactile sensing as formulated in Section II. Solutions to the inverse problem are obtained as the result of asynchronous relaxation of all variables in the network.

We show that the network described satisfies the hypotheses of Theorem 1, which thereby explicitly specifies an energy function for the network. It is shown that the resultant energy function is indeed the variational principle of (8).

Computer simulations of the network are used to evaluate the effect of the regularizing parameter λ on the resultant solutions and to evaluate performance of the network in the presence of sensor noise.

A. The Maximum Entropy Deconvolution Network

Inspired by the work of Tank and Hopfield (see [30]) on neural networks for solving optimization problems, Marrian and Peckerar [31] suggested a neural network for solving deconvolution problems with an entropy-like regularizer. Fig. 3 shows a schematic of a N-channel deconvolution network.

The network proposed consists of two planes of amplifiers: 1) the signal plane and 2) the constraint plane (see Fig. 3). Inputs to the constraint plane ($\epsilon = (\epsilon_1, \ldots, \epsilon_N)^T$) are currents

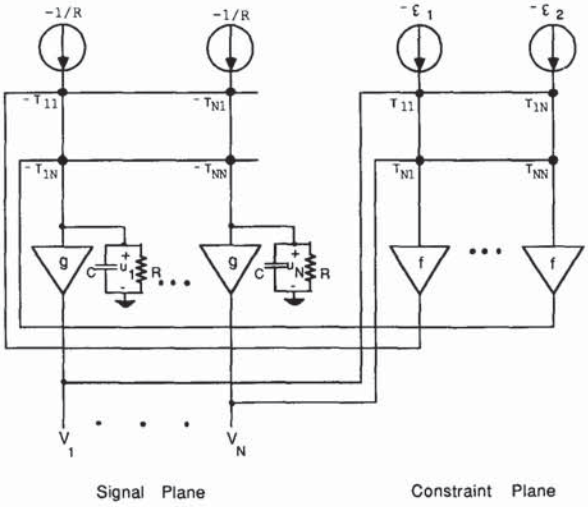

Fig. 3. N-channel maximum entropy deconvolution network.

proportional to sample strain measurements obtained from an array of tactile sensors. Outputs of the signal plane ($u = (u_1, \ldots, u_N)^T$) are voltages that, in equilibrium, represent regularized solutions to the inverse problem. The interconnections T_{ij} are conductances (resistors with values $1/T_{ij}$) corresponding to elements of the matrix representation T of the discretized convolution kernel. Amplifiers in the signal plane are exponential, i.e., $g(x) = \exp(x)$ and constraint plane amplifiers are linear with gain s ($f(x) = sx$). To intuitively understand the manner in which this deconvolution network operates, dynamical evolution of the network can be viewed as occurring in a series of infinitesimal discrete time steps. If evolution of the network is viewed in this manner, the feedback loops generate a number of "analog iterations." Each analog iteration is approximately composed of the following steps:

1) Outputs of the signal plane are convolved with the discretized kernel T in the constraint plane, forming the vector $T \cdot u$.
2) Error in the current estimate of the solution (given by outputs of the signal plane) is evaluated in the constraint plane by subtracting the input strain vector ϵ from the results of the previous step, i.e., the vector $T \cdot u - \epsilon$ is formed and fed back to the signal plane through the constraint plane amplifiers with gain s.
3) Based upon feedback from the constraint plane, the outputs of the signal plane are updated so as to reduce the error.
4) If outputs of the signal plane have not yet settled repeat steps 1)–3).

It remains to be shown that the above series of "iterations" do indeed converge, i.e., that the network, as an analog electrical circuit, is asymptotically stable. Using the results from Section III, we now show that the energy function for the network shown in Fig. 3 corresponds to the variational principle of (8). Thus, stable equilibrium states of the network correspond to regularized solutions to the inverse problem. Since minimization of (8) also involves maximizing the entropy of the solution, we will refer to the network in Fig. 3 as the *maximum entropy deconvolution network* (or MaxEnt network for short).

Stability of the MaxEnt deconvolution network can be established by applying Theorem 1, which also determines explicitly an energy function for the network. In the following, it is assumed that, for the MaxEnt network, any dynamics associated with the constraint plane amplifiers are negligible. This assumption is reasonable since the feedback capacitor associated with the signal plane amplifiers can be chosen so that the response of the signal plane amplifiers is sufficiently slower than those of the constraint plane.

In order to apply Theorem 1, it is necessary to first verify that the network satisfies the two hypotheses. From Fig. 3 it is clear that the voltages across the signal plane capacitors $v_1, \ldots, v_N$ form a complete set of variables for the network, i.e., $v_1, \ldots, v_N$ can be assigned values arbitrarily and that they determine in every branch of the network one of the two variables, branch current or node voltage.

From Fig. 3, the current through the capacitor connected to the nth signal plane node is given by

$$i_n = C\frac{dv_n}{dt} = -\frac{v_n}{R} - \frac{1}{R} - \sum_k t_{kn} f(T_k \cdot u - \epsilon_k). \quad (9)$$

Here, $T_k = (t_{k1}, t_{k2}, \ldots, t_{kN})^T$. It is easily verified from (9) that hypothesis H2 of Theorem 1 is satisfied using $v_1, \ldots, v_N$ as the set of generalized voltage coordinates for the network. Since we are interested in the behavior of the network outputs $u = (u_1, \ldots, u_N)$, we note that u_i are related to v_i by a monotone increasing function $u_i = \exp(v_i) i = 1, \ldots, N$, and apply Corollary 1 to write the energy function for the network in terms of the output variables u.

$$P(u) = -\sum_n \int_0^{u_n} i_n du_n. \quad (10)$$

The dynamical equations of the network can now be written in the following form:

$$\frac{du}{dt} = -GC^{-1}\frac{\partial P(u)}{\partial u} \quad (11)$$

where $u = (u_1 \ldots, u_N)$, $v_n = g^{-1}(u_n)$, $G = \mathrm{diag}(g'(v_1), \ldots, g'(v_N))$, and $C = \mathrm{diag}(C_1, \ldots, C_N)$. Because $g(v) = \exp(v)$ is a monotone increasing function, G is always positive definite. Hence, from (11), it is clear that the equilibrium states of the network must correspond to stationary points of $P(\cdot)$.

In order to understand the nature of the equilibrium states (if any exist) of the network, we must evaluate the integral expression for P.

$$P(u) = \sum_n \int_0^{u_n} \left(\frac{g^{-1}(u_n)}{R} + \frac{1}{R} + \sum_k t_{kn} f(T_k \cdot u - \epsilon_k) \right) du_n$$
$$= \sum_n \int_0^{u_n} \frac{g^{-1}(u_n)}{R} du_n + \sum_n \int_0^{u_n} \frac{du_n}{R}$$

$$+\sum_n \int_0^{u_n} \sum_k t_{kn} f(T_k \cdot u - \epsilon_k) du_n. \quad (12)$$

If we let $F(z_k)$ be such that $dF(z_k)/dz_k = f(z_k)$, then

$$P(u) = \sum_n \int_0^{u_n} \frac{g^{-1}(u_n)}{R} du_n + \sum_n \frac{u_n}{R} + \sum_k F(T_k \cdot u - \epsilon_k). \quad (13)$$

Since the signal plane amplifiers are characterized by $g(u) = \exp(u)$ and the constraint plane amplifiers are characterized by $f(z) = sz$ where s is a constant defining the feedback gain,

$$P(u) = \sum_k \frac{s}{2}(T_k \cdot u - \epsilon_k)^2 + \frac{1}{R}\sum_n u_n \log u_n. \quad (14)$$

It is clear from (14) that $P(u) \to \infty$ as $\|u\| \to \infty$. Hence, all solutions to (11) approach one of the set of equilibrium states as $t \to \infty$.

Equation (14) gives us an explicit form for the energy function for the maximum entropy deconvolution network. In Section II it was noted that there exists a unique minimum of (14) that corresponds to the regularized solution of the inverse problem. Therefore, outputs of the network will converge to a regularized solution of the inverse problem.

Introduction of Other Regularizers: As discussed in Section II, the choice of a regularizing principle must be based upon the physical constraints present in the problem. Also in Section II it was shown that the entropy regularizer is appropriate for the recovery of a stress distribution that is normal to the compliant sensing pad. In the case of tangential stress distributions, use of an entropy regularizer would be inappropriate since tangential stress is not unisense in nature. However, it can be seen from (13) that the network structure described in the last section is not restricted to use with an entropy regularizer only. It is clear that any regularizer that can be written in the form

$$\sum_{i=1}^{N} \int_0^{u_i} g^{-1}(u) du \quad (15)$$

can be introduced into the energy function of the network provided $g(\cdot)$ is a monotone increasing function that can be implemented as the characteristic function of an analog amplifier.

B. Simulations

Computer simulations of the maximum entropy deconvolution network were performed in order to better understand the behavior of the network in terms of speed of convergence, noise immunity, and the effect of the regularizing parameter λ. SIMNON,[4] an interactive simulation program for nonlinear dynamical systems, was used to simulate the network.

For the purpose of simulation, the stress distribution at the surface of the compliant layer was assumed to be the result of applying pressure normal to the surface using a cylindrical object (see Fig. 4). The resulting normal stress distribution due to such a cylindrical indentor can be written as (see [32])

$$f_v(y) = \begin{cases} \frac{p}{\pi a^2}\sqrt{a^2 - y^2} & \text{if } y \in [-a, a] \\ 0 & \text{elsewhere} \end{cases} \quad (16)$$

where p is the force per unit length and a is the halfwidth of the contact region. Simulations were performed using $p = 3$ and $a = 1$. The resulting stress distribution is then convolved with the convolution kernel k_x^v relating normal stress to strain at depth x, given by (2). For the simulations, Poisson's ratio for the material was assumed to be 0.5; the modulus of elasticity $E = 1$ and depth $x = 1$ were used. Samples of the resulting strain are provided as inputs to the network that then attempts to reconstruct the surface stress distribution.

Accurate asessments of convergence time could not easily be made using digital computer simulations. If the signal plane capacitors were assigned values so as to reduce convergence time (by decreasing the RC time constant), numerical instability resulted. By decreasing the integration time step, the problems with instability could be avoided at the cost of tremendous increases in the time necessary to perform a simulation; so it was merely observed at this stage that the network does converge to solutions.

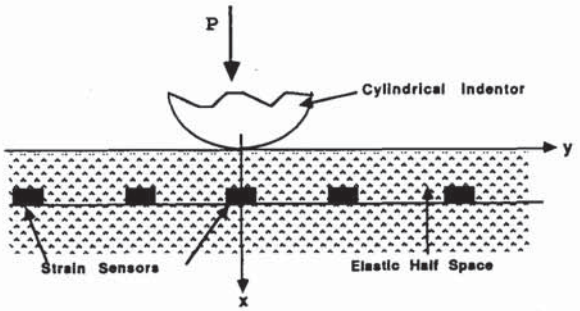

Fig. 4. Application of stress at boundary of elastic half-space using a cylindrical object.

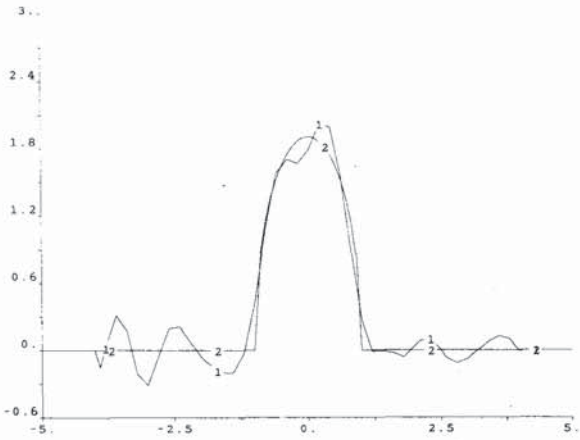

Fig. 5. Network reconstruction of surface stress from noisy strain data ($\sigma^2 = 0.1$) without regularization ($\lambda = 0$) . Curve *1:* Reconstruction. Curve *2:* Designed surface stress.

[4] SIMNON was provided to us by Prof. Astrom from the Lund Institute of Technology.

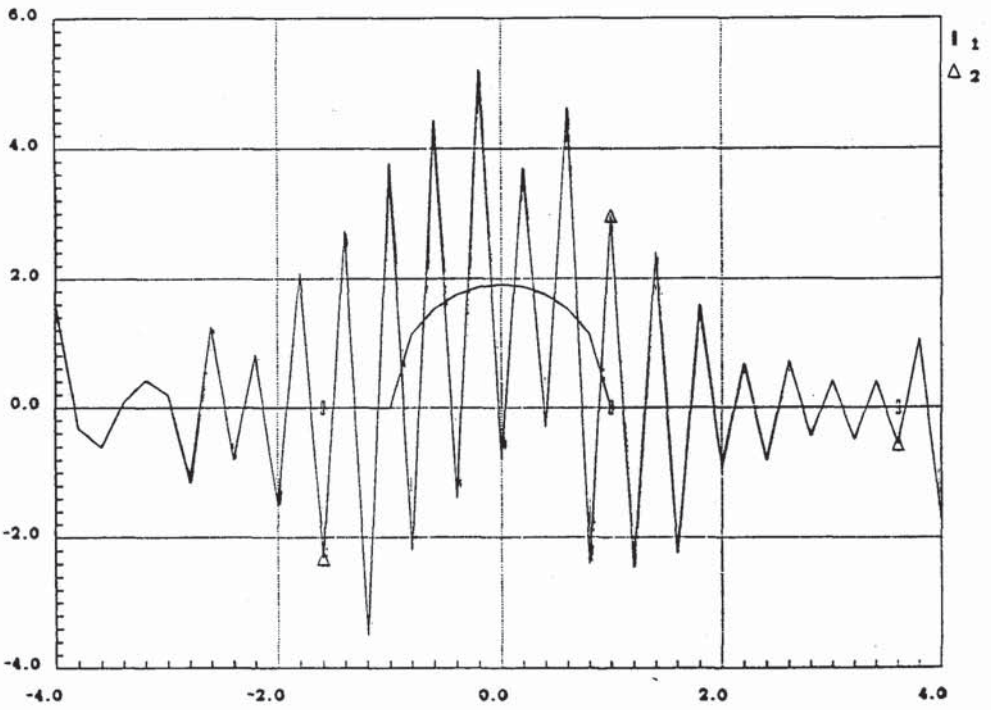

Fig. 6. Reconstruction of surface stress from noisy strain data using the DFT approach. Curve *1:* Designed surface stress. Curve *2:* Reconstruction.

To evaluate performance of the network in the presence of noise, Gaussian white noise with variance σ^2 was added to the strain from which surface stress was to be determined. Fig. 5 shows the reconstruction of surface stress obtained by the network from noisy data ($\sigma^2 = 0.1$) with $\lambda = 0$, i.e., without any regularization. It can be seen that the reconstruction is very poor due to multiple peaks and negative solutions. However, in comparison to the reconstruction obtained under identical conditions using the discrete Fourier transform (see Fig. 6), the network solution is markedly superior.

As the regularizing parameter λ is varied (see Figs. 7 and 8), varying degrees of positivity and smoothness are imposed upon the solution. For $\lambda = 0.1$ (Fig. 7), it is clear that although the solution has been constrained to the positive orthant, the degree of regularization is insufficient for the given noise conditions. In Fig. 8 ($\lambda = 100$), the solution has been over-regularized since solutions that should have been close to zero have been pushed away from zero and the peak of the distribution has been greatly suppressed. Fig. 9 shows reconstruction obtained using $\lambda = 10$, which is the "best" of the three shown.

For given noise conditions and a given set of data for which the solutions are known, a "best" value of the regularizing parameter can be chosen, for example, by minimizing

$$MSE = \frac{1}{N} \sum_i \|f_v^i - \tilde{f}_v^i\|^2$$

where $f_v^i \in \mathbb{R}^N$ are the known solutions for the given data and $\tilde{f}_v^i$ are the solutions provided by the network. However,

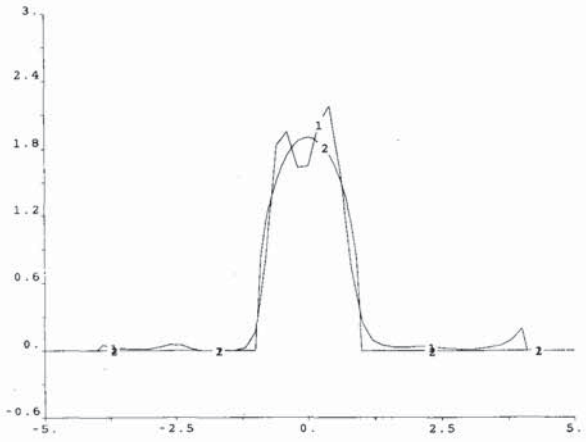

Fig. 7. Network reconstruction of surface stress from noisy strain data for $\lambda = 0.1$. Curve *1:* Reconstruction. Curve *2:* Designed surface stress.

methods of choosing this parameter are still a topic of research, and in general no guarantees can be made as to the performance on data outside the initial test set. Considerable effort has been devoted to this question. See, for instance, the papers of Wahba and others [33], [34] on generalized cross validation; see also Hilgers [35].

1) Discrete Component Prototype of Deconvolution Network: As mentioned earlier, accurate assesments of convergence time for the network are not easily made using digital computer simulations. Also, in analysis of the deconvolution network, it was assumed that any dynamics associated with

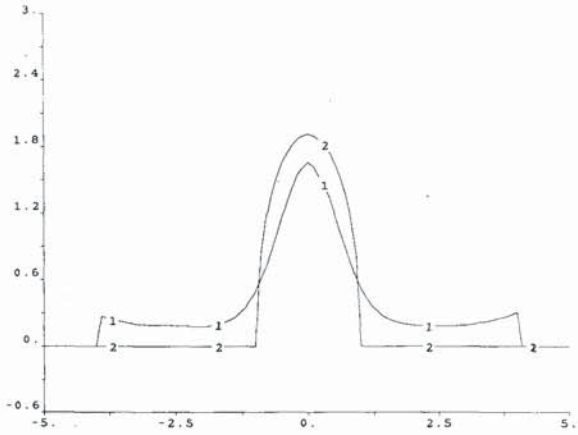

Fig. 8. Network reconstruction of surface stress from noisy strain data for $\lambda = 100$. Curve *1:* Reconstruction. Curve *2:* Designed surface stress.

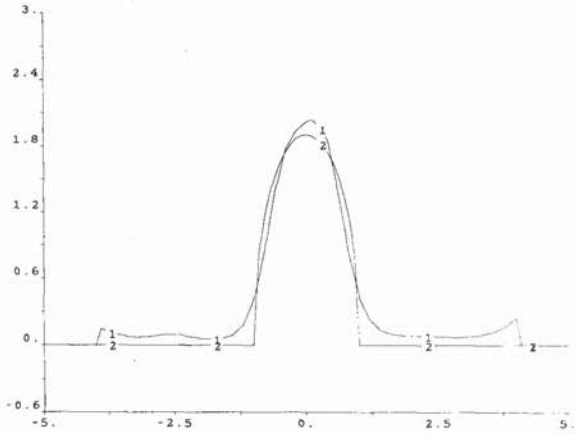

Fig. 9. Network reconstruction of surface stress from noisy strain data for $\lambda = 10$. Curve *1:* Reconstruction. Curve *2:* Designed surface stress.

the constraint plane could be ignored provided that the signal plane amplifiers are sufficiently slower in response. In practical implementations of such a network, it is necessary to understand what effects delays in the constraint plane response may have upon the network. It is ultimately the constraint plane dynamics that limit the achievable speed of convergence. A formal treatment of this subject is to be found in Marcus and Westervelt [36]. A prototype discrete component model of the deconvolution network was constructed using "off-the-shelf" operational amplifiers, resistors, and capacitors. The network was constructed with seven signal plane nodes and seven constraint plane nodes. Since the purpose of constructing the discrete component prototype was to estimate the speed achievable by such a network, exponential amplifiers in the signal plane were replaced by unity gain linear amplifiers to simplify the circuit.[5] Replacing the exponential amplifiers by linear amplifiers results in the entropy regularizer being

[5]A second discrete component prototype was constructed incorporating the exponential amplifiers, but it was used to solve a different problem (see [37]).

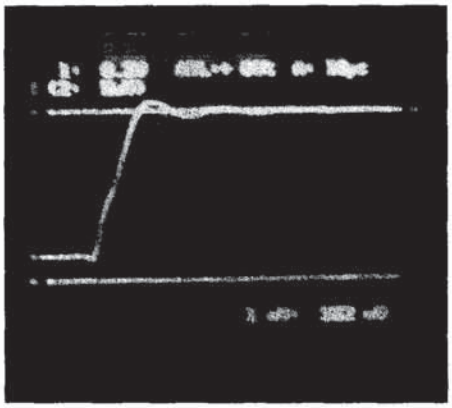

(a)

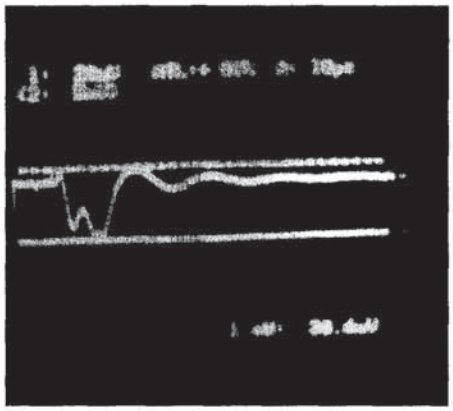

(b)

Fig. 10. Oscilloscope traces showing time evolution of (a) single output of the signal plane and (b) error as measured in the contraint plane, for the seven-channel discrete-component prototype deconvolution network.

replaced by a regularizer of the form

$$\lambda M(v) = \frac{1}{R}\sum_i v_i^2.$$

The interconnection matrix $[T_{ij}]$ was chosen as a seven-point discretization of the elastic kernel $k_x^v(\cdot)$ in (2) and implemented using resistors with values $R_{ij} = 1/T_{ij}$.

Inputs to the network (currents injected into the constraint plane) were chosen to represent samples of the strain distribution due to the compressive loading profile used for the simulations.

The rise time of the constraint plane amplifiers was measured to be approximately 1 μs. The actual response time of the constraint plane would be longer than this since the parallel combination of all resistors connected to the input of any node contribute to the RC time constant. It was observed that for choices of the signal plane capacitors C for which the rise time of the outputs of the network would be below 10 μs, the outputs would oscillate, i.e., the network was unstable. For C=10 pF, the rise time of the outputs of the network was measured to be 10 μs (see Fig. 10). It is clear that the

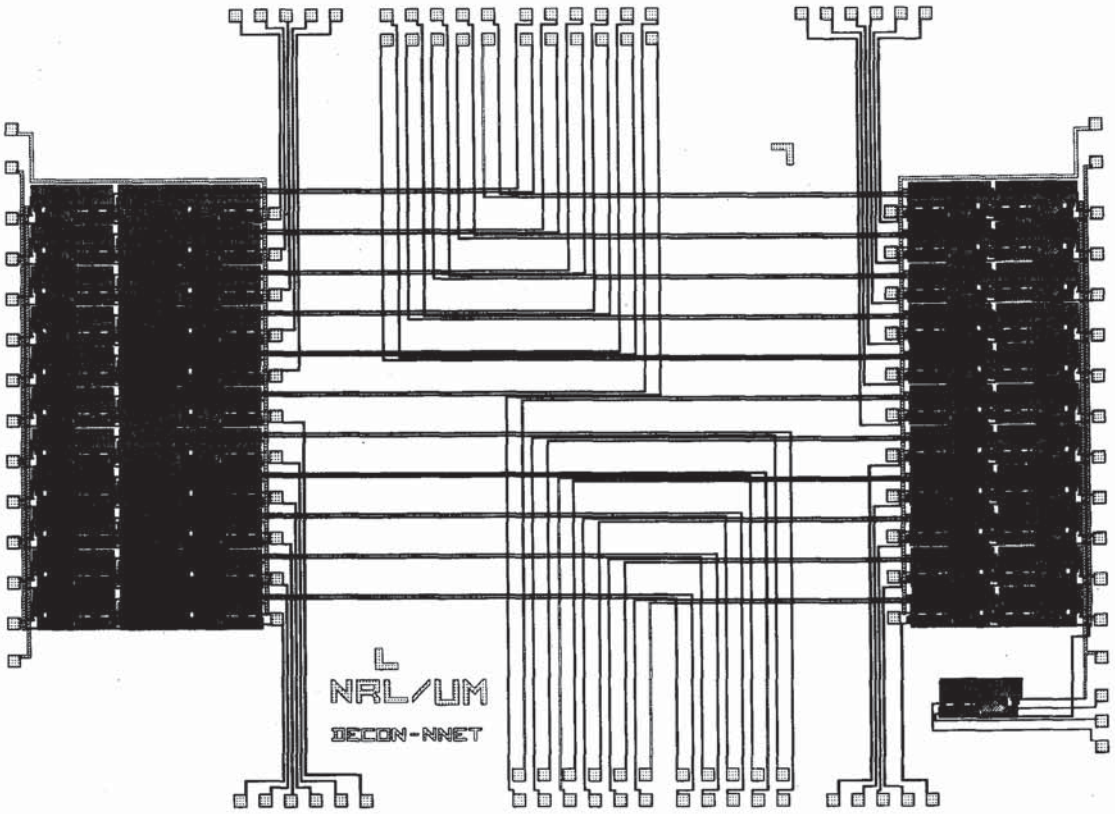

Fig. 11. Layout of integrated circuit chip containing all amplifiers for an eleven channel deconvolution network.

use of faster operational amplifiers would result in an increase in achievable speed since this would decrease the constraint plane response time and thereby permit a decrease in the time constant of the signal plane.

Settling time and overshoot of the outputs of the network are controlled by the gain of the constraint plane nodes. CONSOLE (see [38]) was used to choose a value for the gain so as to minimize overshoot and settling time.

Remarks: First, the risetime of the signal plane amplifiers is governed by RC time constants determined by the signal plane capacitors in parallel with the resistors connected to each node. As the size (number of sensors) of the problem grows, contrary to intuition, computation time actually decreases. This is due to the fact that a larger problem results in a larger matrix, which means more resistors are placed in *parallel* with each capacitor, thereby reducing the RC time constants in the signal plane.

Second, by the above observation and the remark at the end of Section II-B, it is clear that, in the general two-dimensional setting, there are no significant adverse effects upon computational efficiency.

2) Integrated Circuit Prototype: A prototype analog integrated circuit implementation of the deconvolution network described here has been fabricated but remains to be tested. A hierarchical design philosophy is practiced in this initial implementation. The deconvolution network may be thought of as composed of two sections: 1) active components of the network including signal and constraint plane amplifiers and 2) the functionally passive[6] resistive interconnection matrix. These two sections may also be thought of in the following manner. Once the size of the deconvolution network (number of inputs and outputs) has been decided, the amplifiers of the network are determined. However, the resistive matrix may be a variable entity. For instance, given two different elastic materials (or even two different thicknesses of a given elastic material), the convolution kernel $k_x^v(\cdot)$ and hence its discretization $[T_{ij}]$ are, in general, different. Thus, the network may be thought of as being composed of a fixed part and a variable part.

If fixed resistors are to be used to implement the interconnect matrix, then some provision should be made to change this matrix without having to refabricate the rest of the network. In order to provide some flexibility in the choice of the interconnect matrix and to permit the use of two different fabrication technologies, the deconvolution network was fabricated as two separate integrated circuits.

The amplifier chip (shown in Fig. 11) is designed to serve as the "motherboard" for the network on top of which the

[6]The term "functionally passive" here is used to describe the fact that in some situations it is desirable to use active circuit components configured to look like a passive resistor from an input/output standpoint.

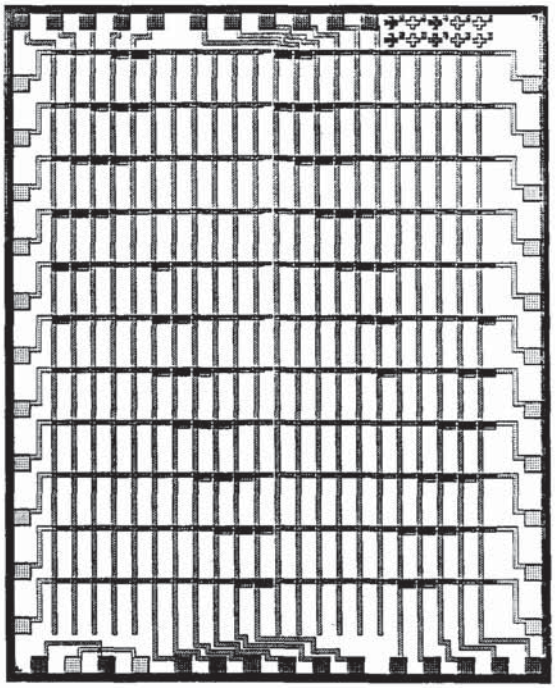

Fig. 12. Layout of resistive interconnection matrix chip.

resistive connection matrix chip (see Fig. 12). Connections between the two chips are made by local wire bonds between bonding pads provided for this purpose on both chips. This approach also facilitates experimentation with different types of connection matrices such as those with programmable connections.

V. Conclusions

In this paper, we considered the inverse problem of recovering stress distributions over regions of contact from samples of strain provided by an array of tactile sensors. In the case where stress is applied to the surface of a compliant material and strain is measured at a fixed depth beneath the surface, the inverse problem was shown to be a problem of deconvolution. It was shown that the technique of regularization could be used to introduce *a priori* knowledge into the problem in order to obtain solutions. The constraints of nonnegativity and smoothness were imposed by choosing an entropy regularizer for the recovery of normal surface stress. Solutions to the inverse problem could then be obtained by minimization of a cost functional. We demonstrated that, under certain hypotheses, energy functions may be explicitly determined for nonlinear RC electrical networks. Stable equilibria of the network were shown to correspond to local minima of the energy function and conditions for stability of the network were determined.

An analog neural network for regularized solution of the inverse problem was proposed. Using the results of Section III, it was shown that the energy function of the proposed network corresponds to the variational principle formulated for solution of the inverse problem of tactile sensing. Stability of the network, in terms of electrical circuit analysis, was guaranteed by the monotonicity of the characteristics of the signal plane amplifiers. It was also determined that any regularizer that could be written in the form of (15) and satisfied the monotonicity requirements for the signal plane amplifier characteristic g could be incorporated into the energy function for the network. Computer simulations demonstrated the ability of the deconvolution network to accurately recover normal surface stress even when the sensor outputs were severely corrupted by noise.

A breadboard prototype of the deconvolution network was used to demonstrate the computational speed achievable by such a hardware implementation. Convergence time for the breadboard prototype was measured to be approximately 10 μs. An integrated circuit implementation of the proposed deconvolution network was undertaken. A hierarchical approach was taken in the integrated circuit implementation to provide flexibility in the design of an interconnection matrix.

VI. Discussion

Most early vision problems are ill posed, and regularization has successfully been applied in solving many of them (see, e.g., [18] and [4]). However, regularization as a technique for solving ill-posed problems has also demonstrated limitations. Among the limitations of standard regularization theory is its inability to effectively cope with discontinuities [39]. If the operators K and P in (5) are linear (as in standard regularization theory), the solution space is essentially restricted to generalized splines. Hence, in some cases the resultant solutions will be overly smooth and cannot be trusted at discontinuities such as edges. A number of approaches have been suggested to overcome some of the limitations of standard regularization theory. Examples of some of these approaches can be found in [40]–[42], [39], and [18]. Such approaches often result in nonquadratic variational priciples.

It is clear that the class of problems for which quadratic variational principles are sufficient is limited. For every quadratic variational principle, it can be shown that there exists a corresponding linear analog electrical network consisting of resistors, voltage sources, and current sources that has the same solutions. This fact is used in [4] to synthesize analog resistive networks to solve problems in early vision. In [43], the approach taken to solving a nonquadratic variational principle employs a hybrid analog-digital network that at each iteration (on the digital time scale) solves a quadratic variational principle (in analog). In general, nonquadratic variational principles may posses numerous local minima in addition to global minima. The deterministic gradient descent approach taken in [43] demonstrated an ability to perform well (qualitatively) in comparison to statistical annealing that converges to the global solution with probability one if appropriately applied. However, convergence to the global solution cannot be guaranteed, and the hybrid analog-digital nature of the network introduces additional hardware complexity.

In this paper, it was shown that a strictly analog network can be structered so as to solve a nonquadratic variational

principle. Convergence to the global solution, in this case, is guaranteed since the variational principle of (8) is strictly convex. It was also shown that there exists a class of nonquadratic variational principles (see (15)) that can be solved by similar networks by choosing appropriate characteristics $g(\cdot)$ for the signal plane amplifiers. In the case of this larger class of nonquadratic variational principles, convergence to global solutions cannot in general be guaranteed.

So far the discussion in this paper has been confined primarily to the problems of early taction. The highest level of the tactile sensing hierarchy, which has been ignored so far, is crucial to the usefulness of any tactile sensing system. A higher level description of the tactile environment is the next step beyond the low-level description provided by the processes of early taction. For instance, although a low-level description of a grasped object may be sufficient to secure the object in a stable grasp, it is not adequate to directly identify the object. In this aspect of tactile sensing as well, neural networks may provide a solution. Adaptive neural networks have demonstrated a remarkable ability to "learn" complex representations and successfully classify patterns based on these representations (cf. [44]–[46]) [51].

It was shown by construction of a breadboard circuit that analog hardware implementation of the proposed network leads to convergence times in the order of 10μs. In order to compare this with digital computation, we note that simple inversion of an $n \times n$ symmetric Toeplitz matrix is of computational complexity $O(n^2)$. For the purpose of a biased comparison (biased in favor of digital computation), we can ignore the regularizer and assume that it takes exactly n^2 operations to invert the matrix A. Then for a modest 5×5 array of tactile sensors it would be necessary to perform

$$25^2 \frac{\text{operations}}{\text{solution}} \times 10^5 \frac{\text{solutions}}{\text{second}} = 62.5 \frac{\text{million operations}}{\text{second}}$$

in order to keep up with the processing speed of the analog network. This is clearly not possible for local digital computation. Also, as the size of the sensor array increases, the processing time required for digital computation increases quadratically. It was noted in Section IV-B that, in the case of the analog network, convergence time actually decreases as the size of the problem increases. In [2] it was established through survey that processing times of approximately 1–2 ms are sufficiently fast for most tactile sensing applications. Additional available time resulting from the use of analog network processors could be utilized to perform other tasks such as predicting slippage based upon prior and current processing results.

Appendix A
Ill Posedness of the Inverse Problem of Tactile Sensing

The general form of integral equations of the first kind is given by

$$g(t) = \int_a^b k(t,s) f(s) ds, \qquad c \le t \le d. \tag{A1}$$

Equation (A1) may be rewritten in operator notation as

$$g(t) = (Kf)(t) \tag{A2}$$

where K is the integral operator with kernel function k. In the particular case of the tactile sensing problem, K is a convolution operator with the convolution kernel k. Since $g(\cdot)$ and $f(\cdot)$ in this case represent strain and stress, respectively, and are therefore signals with finite energy, we consider the case where $g, f \in L_2([a,b])$ with norm defined by

$$\|h\|_2 = \left(\int_a^b |h(x)|^2 dx \right)^{1/2} \tag{A3}$$

and $a = y_{\min}, b = y_{\max}$. Thus, we are interested in the case when $k_x(y, y_0)$[7] $\in L_2([a,b] \times [a,b])$ and

$$p_x(y) = (Kq_v)(y) = \int_a^b k_x(y, y_0) q_v(y_0) dy_0. \tag{A4}$$

To demonstrate the ill-posed nature of the inverse problem, we would like to

1) show that in the infinite dimensional setting of (A4) the inverse of the integral operator K is unbounded and
2) show that the finite dimensional manifestation of the unboundedness of the inverse of K occurs in the ill conditioning of the finite matrix approximation of the operator K.

It is easily shown that the integral operator K is bounded, linear, self-adjoint, and compact (see [47]). Although every linear operator on a finite dimensional Hilbert space over $\mathbb{C}$ has an eigenvalue, it is not true that even a self-adjoint operator on an infinite dimensional Hilbert space must have an eigenvalue. The next two theorems[8] are concerned with the eigenvalues of such operators.

Theorem 2:

a) Any eigenvalue of a self-adjoint operator is real.

b) If λ is an eigenvalue of $A \in L(H)$, then $|\lambda| \le \|A\|$.

c) If $A \in L(H)$ is compact and self-adjoint, then A has an eigenvalue and at least one of the numbers $\|A\|$ or $-\|A\|$ is an eigenvalue of A. ■

Theorem 3: Let $A \in L(H)$ be a compact self-adjoint operator, where H is an infinite dimensional Hilbert space. Then the spectrum $\sigma(A)$ of A consists of zero and the eigenvalues of A. $(0 \in \sigma(A))$ ■

Now $(\lambda I - K)$ is invertible for $\lambda \notin \sigma(K)$. Since K is compact and self adjoint, by Theorem 3, $0 \in \sigma(K)$. Hence, the inverse of $(\lambda I - K)$ is unbounded for $\lambda = 0$, which is equivalent to saying that the inverse of the integral operator K is unbounded.

From the above result, it is clear that, in the infinite dimensional case, the inverse problem is ill posed in the sense of Hadamard since the inverse of the operator K is unbounded; solutions will not depend continuously upon the initial data.

Finite Matrix Approximation of the Convolution Kernel: In the context of the tactile sensing problem, the convolution operator K has been approximated by a finite rank operator by discretizing the kernel k and considering only samples of the stress and strain. The use of such an approximation is justified since every compact operator in $L(H_1, H_2)$ is the

[7] We will use $k_x(y, y_0)$ to denote $k_x^v(y, y_0)$ unless otherwise indicated.

[8] For proofs of these theorems, see [47] and/or [48].

limit, in norm, of a sequence of operators of finite rank. Let $A = [a_{ij}]$ be a (infinite) matrix representation of the operator K. Since $0 \in \sigma(K)$ and A is unitarily equivalent to K, zero is also in the spectrum of A. Let $\widetilde{K}_n$ (of rank n) with finite matrix representation $\widetilde{A}_n$ be a finite rank approximation to K. As $n \to \infty$ the approximation becomes better; however, since $0 \in \sigma(K)$ as $n \to \infty$, at least one of the eigenvalues of $\widetilde{A}_n$ approaches zero. By Theorem 2, at least one of the eigenvalues of $\widetilde{A}_n$ approaches either $\|K\|$ or $-\|K\|$.

The condition number $P(A)$ of a matrix A is defined as

$$P(A) = \frac{\max\limits_{j} |\lambda_j(A)|}{\min\limits_{j} |\lambda_j(A)|}. \tag{A5}$$

In solving a finite system of linear equations of the form $Ax = y$, the condition number is a measure of the sensitivity of solutions to errors in the initial data y and approximations made in the inversion of the matrix A (e.g., finite word length effects) on the solution x. Large values of $P(A)$ result in large errors in the solution. In the event that $P(A)$ is large ($P(A) = 1$ being the best case), we say that the matrix A is "ill conditioned."

It is clear from the observations made earlier about the eigenvalues of $\widetilde{A}_n$ that, as $n \to \infty$, $\widetilde{A}_n$ becomes increasingly ill conditioned since the denominator in (A5) approaches zero while the numerator approaches $\|K\|$.

We have shown that, in the infinite dimensional case, the inverse problem is ill posed in the sense of Hadamard. The ill posedness of the problem in this case is due to the unboundedness of the inverse of the integral operator K, which is in violation of Hadamard's third requirement that the solution depend continuously on the initial data for the problem to be well posed. We have also made the observation that unboundedness of the inverse of K induces ill conditioning of the finite matrix approximation to K.

Appendix B
Energy Functions for Nonlinear *RC* Electrical Networks: Definitions Pertaining to Nonlinear Networks

Elements: Two terminal elements can in general be described by a relationship of the form

$$f(i, \frac{di}{dt}, \frac{d^2i}{dt^2}, \ldots, v, \frac{dv}{dt}, \frac{d^2v}{dt^2}, \ldots, t) = 0 \tag{B1}$$

where v is the voltage across the two terminals of the element and i is the current through the element.

Nonreactive elements are those for which the dependence on time derivatives in (B1) is absent, i.e., they can be described by $f(i, v, t) = 0$.

Time invariant elements are those for which the defining function is not explicitly time dependent.

For time-invariant nonreactive elements the locus of $f(i, v) = 0$ is called the *characteristic curve* of the element. For general time-invariant elements, the $i-v$ curve represents a trajectory in the phase space of the element viewed as a dynamical system.

A time-invariant nonreactive element is said to be *passive* if the characteristic curve intersects the $i-v$ axes at no point other than the origin. Otherwise, the element is said to be *active*.

Sources: A current–voltage source is a time-invariant active nonreactive element for which voltage/current is absent from the defining function $f(i, v)$.

Among the first theorems for linear electrical networks is Maxwell's Minimum Heat Theorem (1837), which is stated below in modern terminology.

Theorem 4—Maxwell's Minimum Heat Theorem: For any linear, time-invariant, resistive network driven by voltage and/or current sources, of all the current distributions consistent with Kirchoff's current law, the only distribution also consistent with Kirchoff's voltage law and therefore the true distribution is the one that minimizes the quantity $(W - 2P_v)$ where W is the total power dissipated by the resistors and P_v is the total power supplied by the voltage sources. ■

Having chosen a set of generalized current coordinates, say for example, $i_1, \ldots, i_m$, Maxwell's theorem leads to the following set of m equation:

$$\frac{\partial}{\partial i_j}(W - 2P_v) = 0, \qquad j = 1, \ldots, m \tag{B2}$$

which, when solved for the current coordinates $i_1, \ldots, i_m$, determine all variables in the network.

The dual of Maxwell's theorem states that for the above network, among all voltage distributions that are consistent with Kirchoff's voltage law, the only one also consistent with Kirchoff's current law and therefore the true distribution is the one that minimizes $(W - 2P_I)$, where P_I is the total power supplied by the current sources. This dual theorem can be used to solve for all variables in the network by first solving for the generalized voltage coordinates.

Maxwell's theorem tells us that the quantities $(W - 2P_v)$ and $(W - 2P_I)$ are stationary with respect to the distributions of currents and voltages in the network, respectively. It can be shown that these quantities are not in general stationary in the case of networks containing nonlinear elements. Hence, to solve for voltages and currents in a nonlinear network in an analogous manner we must determine first the stationary quantities.

Invariants of Motion in Nonlinear Electrical Networks

Two quantities defined by Millar [22] relating to elements of a nonlinear network are the "content" and the "co-content" of an element.

Content and Co-content: Let (i_1, v_1) be a point on the $i-v$ curve of a two-terminal element. The "content" of the element, denoted by G, is defined by

$$G = \int_0^{i_1} v di. \tag{B3}$$

The "co-content" of the element is denoted by J and is defined by

$$J = \int_0^{v_1} i dv. \tag{B4}$$

We observe that for a passive element the total power dissipation is $W = J+G$ and that for a linear, passive element $J = G = W/2$

The total content (co-content) of a network is defined as the sum of contents (co-contents) of all constituent elements including current and voltage sources. We will use G and J to denote the total content and co-content, respectively. We will use G_{jk} and J_{jk} to denote the content and co-content of the element connecting nodes j and k.

Stationary Quantities: The following theorem identifies G and J as stationary quantities.

Theorem 5 (Millar): If in an active (possibly reactive) network the sum J of the co-contents of all the constituent elements is expressed in terms of the defining number of voltage coordinates of the network subject only to the restrictions of Kirchoff's voltage law, then J is stationary for the actual distribution of voltages. ∎

The dual of this theorem is obtained by replacing co-content by content, J by G, and voltage by current everywhere.

Theorem 5 provides us with the equivalent of Maxwell's theorem for nonlinear networks of time-invariant elements. To restate the above theorem in a manner analogous to Maxwell's theorem, we can say the following:

In any active (possibly reactive) network, of all distributions of current/voltage consistent with Kirchoff's current/voltage law, the ones for which G/J is stationary are the only ones that are also consistent with Kirchoff's voltage/current law and are thereby the true distributions.

Thus, if we express G/J in terms of the defining number (m/n) of current/voltage coordinates, we can determine all currents and voltages in the network by solving either one of the following sets of simultaneous partial differential equations $\delta G/\delta i_r = 0,\ r = 1,\ldots,m$, or $\delta J/\delta v_q = 0,\ q = 1,\ldots,n$.

Invariants of Motion: The next theorem identifies G and J as invariants of motion. That is, as a network evolves in time following an impulsive change in one or more of the current or voltage sources, the total content and the total co-content of the network are conserved.

Theorem 6 (Millar): In any network of time-invariant elements (possibly including sources), the total content G and the total co-content J are invariants of motion (i.e., $dG/dt = 0$ and $dJ/dt = 0$, where dG/dt and dJ/dt are the total time derivatives of G and J given by

$$\frac{dG}{dt} = \frac{\partial G}{\partial t} + \frac{\partial G}{\partial i_1}\frac{di_1}{dt} + \cdots + \frac{\partial G}{\partial i_m}\frac{di_m}{dt}$$

and

$$\frac{dJ}{dt} = \frac{\partial J}{\partial t} + \frac{\partial J}{\partial v_1}\frac{dv_1}{dt} + \cdots + \frac{\partial J}{\partial v_n}\frac{dv_n}{dt}$$

where m is the defining number of generalized current coordinates and n is the defining number of generalized voltage coordinates. ∎

In a directed network with b branches and m nodes, the set of branch currents $i = (i_1,\ldots,i_b)$ and the set of branch voltages $v = (v_1,\ldots,v_b)$ are vectors in a b-dimensional Euclidean vector space $\mathcal{E}^b$ with the inner product defined by $\langle x,y\rangle = \sum_{\mu=1}^{b} x_\mu y_\mu$. Let $\mathcal{I}$ be the set of all vectors in $\mathcal{E}^b$ such that if $i \in \mathcal{I}$, then the constraint of Kirchoff's current law is satisfied for each node in the network, i.e., $\sum_{\text{node}} i_\mu = 0$. Similarly, let $\mathcal{V}$ be the set of all vectors in $\mathcal{E}^b$ such that if $v \in \mathcal{V}$, then Kirchoff's voltage law is satisfied, i.e., $\sum_{\text{loop}} v_\mu = 0$. $\mathcal{I}$ and $\mathcal{V}$ are clearly subspaces of $\mathcal{E}^b$ since they are defined via linear relationships (Kirchoff's laws). The following theorem, which appears in [23], is easily obtained using Tellegen's theorem (see [20]), which states that $\mathcal{I}$ and $\mathcal{V}$ are orthogonal subspaces of $\mathcal{E}^b$.

Theorem 7 (Brayton–Moser): Let Γ denote a one-dimensional curve in $\mathcal{I}\times\mathcal{V}$ with coordinates denoted by i and v. Then

$$\int_\Gamma \sum_{\mu=1}^{b} v_\mu di_\mu = \int_\Gamma \sum_{\mu=1}^{b} i_\mu dv_\mu = 0. \quad \blacksquare \qquad \text{(B5)}$$

Having stated the above two theorems and having defined the complete set of variables $v* = (v_1,\ldots,v_N)$ for the network, we proceed with the proof of Theorem 1

Proof of Theorem 1: From Theorem 7 we know that $\int_\Gamma \sum_{\mu=1}^{b} i_\mu dv_\mu = 0$. We choose Γ from a fixed initial point to a variable end point in $\mathcal{E}^b$ such that along Γ the characteristic relationships of the constituent elements of the network are satisfied. We can write (B5) in the following form:

$$\int_\Gamma \sum_{\rho=1}^{N} i_\rho dv_\rho + \int_\Gamma \sum_{\mu=N+1}^{b} i_\mu dv_\mu = 0. \qquad \text{(B6)}$$

The first integral is over all capacitive branches, and the second is over all other branches. Note that if the first integral on the left is independent of the path Γ then the integration and summation may be interchanged to obtain $-P(v)$ as defined in the statement of Theorem 1. Let

$$\tilde{P}(v) = -\int_\Gamma \sum_{\rho=1}^{N} i_\rho dv_\rho. \qquad \text{(B7)}$$

Let $\xi = \sum_{\rho=1}^{N} i_\rho dv_\rho$. For the integral in (B7) to be independent of Γ, it is necessary that ξ be a perfect differential. That is, we can write ξ as $\xi = d\sigma$, where $\sigma = \sigma(v_1,\ldots,v_N)$ and

$$d\sigma = \frac{\partial\sigma}{\partial v_1}dv_1 + \cdots + \frac{\partial\sigma}{\partial v_N}dv_N. \qquad \text{(B8)}$$

But since we want $\xi = d\sigma$, we must have $d\sigma = i_1dv_1 + \cdots + i_Ndv_N$. Equivalently, we need $i_\rho = \delta\sigma/\delta v_\rho,\ \rho = 1,\ldots,N$, which is the case *if and only if*

$$\frac{\partial i_\rho}{\partial v_\eta} = \partial^2\sigma\frac{\partial v_\rho}{\partial v_\eta} = \frac{\partial i_\eta}{\partial v_\rho}, \quad \eta,\rho = 1,\ldots,N. \qquad \text{(B9)}$$

By hypothesis H2, (B9) holds. Hence, $\tilde{P}(v)$ is a function of the endpoints of Γ alone, and choosing the origin as a starting point for Γ, we have

$$\tilde{P}(v) = P(v) = -\sum_{n=1}^{N}\int_0^{v_n} i_n dv_n. \qquad \text{(B10)}$$

In this case we have

$$i_\rho = -\frac{\partial P(v)}{\partial v_\rho} = C_\rho\frac{dv_\rho}{dt}, \quad \rho = 1,\ldots,N \qquad \text{(B11)}$$

where the equality on the right is obtained by the dynamical law of capacitors.

Therefore

$$C_\rho \frac{dv_\rho}{dt} = -\frac{\partial P(v*)}{\partial v_\rho}, \quad \rho = 1, \ldots, N \qquad \text{(B12)}$$

where $v* = (v_1, \ldots, v_N)$. We now write the system of differential equations defining the dynamical behavior of the network in the following vector form:

$$-C\dot{v^*} = \frac{\partial P(v^*)}{\partial v^*} \qquad \text{(B13)}$$

where $C = \text{diag}(C_1, \ldots, C_N)$, and $\delta P(x)/\delta x$ is the gradient of $P(x)$. Since the matrix C is positive definite and symmetric, we know that $(d/dt)P(v^*(t)) \leq 0$ and $(d/dt)P(v^*(t)) = 0$ if and only if v^* is an equilibrium of the gradient system (B13). Hence, if $\tilde{v^*}$ is an isolated minimum of $P(v^*)$, then $\tilde{v^*}$ is an asymptotically stable equilibrium of the gradient system (B13).

Therefore, the equilibrium states of the network correspond to stationary points of $P(v^*)$, which we shall call the energy function, and the local minima of $P(v^*)$ are the stable equilibria of the network. If in addition to this $P(x) \to \infty$ as $\|x\| \to \infty$, then it can be shown using a well known result from Lyapunov stability theory that all solutions to (B13) approach one of the set of equilibrium solutions as $t \to \infty$. ■

We observe that $P(v*)$ is just the negative of the co-content of *all independent capacitive branches* in the network. The total co-content of the network, J, is an invariant of motion (Millar [22]) even for dissipative systems where the total energy is not conserved. The analogy to kinetic and potential energy of a nondissipative mechanical system is evident. $P(v*)$ can be regarded as a type of potential energy that is minimized as the system settles. The sum of the co-contents of all other branches in the network plays the role of kinetic energy. J, the sum of these two quantities, is like the total energy of the system and is conserved.

REFERENCES

[1] G. Gordon, Ed., *Active Touch*. Oxford, England: Pergamon, 1978.

[2] L. Harmon, "Automated tactile sensing," *Int. J. Robotics Res.*, vol. 1, no. 2, pp. 3–32, 1982.

[3] C. Mead and M. Ismail, *Analog VLSI Implementation of Neural Systems*. New York: Kluwer, 1989.

[4] T. Poggio and C. Koch, "Ill-posed problems in early vision: from computational theory to analogue networks," *Proc. R. Soc. London*, vol. B 226, pp. 303–323, 1985.

[5] J. Hadamard, *Lectures of the Cauchy Problem in Linear Partial Differential Equations*. New Haven, CT: Yale Univ. Press, 1923.

[6] M. Lee and H. Nichols, "A survey of robot tactile sensing technology," *Int. J. Robotics Res.*, June 1989.

[7] P. Dario, D. DeRossi, C. Domenici, and R. Francesconi, "Ferroelectric polymer tactile sensors with anthropomorphic features," in *Proc. Int. Conf. Robotics* (Atlanta, GA, Mar. 13–15, 1984), pp. 332–339.

[8] C. T. Yao, M. C. Peckerar, J. Wasilik, C. Amazeen, and S. Bishop, "A novel three dimensional microstructure fabrication technique for a triaxial sensor." Preprint, Naval Res. Lab., Code 6804, Washington, DC, 1987.

[9] D. Mott, M. Lee, and H. Nichols, "An experimental very high resolution tactile sensor array," in *Proc. 4th Int. Conf. Robot Vision Sensory Control* (London), 1984.

[10] J. J. Clark, "A magnetic field based compliance matching sensor for high resolution, high compliance tactile sensing," in *Proc. IEEE Int. Conf. Robotics Automat.*(Philadelphia, PA), Apr. 1988, pp. 772–777..

[11] R. W. Brockett, "Stability and control of grasping." presented at IEEE Conf. Robotics Automat., 1986.

[12] S. Timoshenko and J. Goodier, *Theory of Elasticity*. New York: McGraw-Hill, 1951.

[13] R. Yang, "Tactile perception for multifingered hands," Master's thesis, Univ. of Maryland, College Park, 1987; also Systems Res. Center Tech. Rep. SRC-TR-87–126.

[14] R. Fearing and J. Hollerbach, "Basic solid mechanics for tactile sensing," *Int. J. Robotics Res.*, vol. 4, no. 3, 1985.

[15] R. Fearing and T. Binford, "Using a cylindrical tactile sensor to determine curvature," in *Proc. IEEE Int. Conf. Robotics Automat.* (Philadelphia, PA), Apr. 1988, pp. 765–771.

[16] A. Tikhonov, "Solution of incorrectly formulated problems and the regularization method," *Sov. Math. Dokl*, vol. 4, pp. 1035–1038, 1963.

[17] A. Tikhonov and V. Arsenin, *Solutions of Ill Posed Problems*. Washington, DC: Winston Press, 1977.

[18] T. Poggio, V. Torre, and C. Koch, "Computational vision and regularization theory," *Nature*, vol. 317, no. 6035, pp. 314–319, 1985.

[19] J. C. Maxwell, *A Treatise on Electricity and Magnetism*, 3rd ed., vol. I. New York: Dover, 1954, p. 407.

[20] B. Tellegen, "A general network theorem with applications," *Phillips Res. Rep.*, vol. 7, 1952.

[21] C. Cherry, "Some general theorems for nonlinear systems possesing reactance," *Phil. Mag.*, vol. 42, pp. 1161–1177, 1951.

[22] W. Millar, "Some general theorems for nonlinear systems possessing resistance," *Phil. Mag.*, vol. 42, pp. 1150–1160, 1951.

[23] R. Brayton and J. Moser, "A theory of nonlinear networks i and ii," *Quart. Appl. Math.*, vol. 22, nos. 1 and 2, pp. 1–33, 81–184, 1964.

[24] T. Matsumoto, "On several geometic aspects of nonlinear networks," *J. Franklin Inst.*, vol. 301, nos. 1 and 2, 1976.

[25] C. Desoer and F. Wu, "Trajectories of nonlinear rlc networks: A geometric approach," *IEEE Trans. Circuit Theory*, vol. CT-19, no. 6, pp. 562–571, 1972.

[26] T. Matsumoto, "On dynamics of electrical networks," *J. Differential Equations*, vol. 21, no. 1, pp. 179–196, 1976.

[27] T. Matsumoto, "Eventually passive nonlinear networks," *IEEE Trans. Circuits Syst.*, vol. CAS-24, no. 5, pp. 261–269, 1977.

[28] S. Smale, "On mathematical foundations of electrical circuit theory," *J. Differential Geometry*, vol. 7, pp. 193–210, 1972.

[29] Y. C. Pati, "Neural networks for low-level processing of tactile sensory data," Master's thesis, Univ. of Maryland, College Park, 1988; also Systems Res. Center Tech. Rep. SRC-TR-89–8.

[30] D. Tank and J. Hopfield, "Simple 'neural' optimization networks: An a/d converter, signal decision circuit and a linear programming circuit," *IEEE Trans. Circuits Syst.*, vol. CAS-33, no. 5, pp. 533–541, 1986.

[31] C. Marrian and M. Peckerar, "Electronic neural net algorithm for maximum entropy deconvolution," in *Proc. IEEE 1st Ann. Int. Conf. Neural Networks* (San Diego, CA), June 1987.

[32] H. Conway *et al.*, "Normal and shearing contact stress in indented strips and slabs," *Int. J. Eng. Sci.*, vol. 4, pp. 343–359, 1966.

[33] G. Wahba, "Ill posed problems: Numerical and statistical methods for mildly, moderately and severely ill posed problems with noisy data," Tech. Rep. 595, Dept. of Statistics, Univ. of Wisconsin, Madisson, Feb. 1980.

[34] D. M. Bates, M. J. Lindstrom, G. Wahba, and B. S. Yandell, "GCVPACK — Routines for generalized cross validation," *Commun. Statist.-Simula.*, vol. 16, no. 1, pp. 263–297, 1987.

[35] J. Hilgers, "Non-iterative methods for solving operator equations of the first kind," Tech. Rep. TSR 1413, Math. Res. Center, Univ. of Wisconsin, Madison, 1974.

[36] C. Marcus and R. Westervelt, "Stability of analog neural networks with delay," *Press. Phys. Rev. A.*, vol. 39, no. 1, p. 347, 1989.

[37] C. R. K. Marrian, M. C. Peckerar, I. Mack, and Y. C. Pati, "Electronic 'neural' nets for solving ill-posed problems with an entropy regularizer," in *Maximum Entropy and Bayesian Methods*, J. Skilling, Ed. New York: Kluwer, 1989, pp. 371–376.

[38] M. Fan, J. Koninckx, L. Wang, and A. Tits, "Console: A CAD tandem for optimization-based design interacting with arbitrary simulators," Tech. Rep., Univ. of Maryland, Systems Res. Center, 1987.

[39] J. Marroquin, S. Mitter, and T. Poggio, "Probabilistic solution of ill-posed problems in computational vision," *J. Amer. Statistical Assoc.*, vol. 82, no. 397, pp. 76–89, 1987.

[40] D. Terzopoulus, "Multiresolution computation of visible-surface representation," Ph.D. dissertation, Dept. of Electrical Eng. Comput. Sci., Masachusettes Institute of Technology, Cambridge, 1984.

[41] J. Marroquin, Memo 792, MIT, Artificial Intell. Lab, 1984.

[42] ——, "Probabilistic solution of inverse problems," Tech. Rep. 860, MIT, Artificial Intell. Lab., 1985.

[43] J. Hutchinson, C. Koch, J. Luo, and C. A. Mead, "Computing motion using analog and binary resistive networks," *IEEE Computer Mag.*, pp. 52–63, Mar. 1988.

[44] H. P. Graf, L. D. Jackel, and W. E. Hubbard, "VLSI implementation of a neural network model," *IEEE Computer Mag.*, pp. 41–49, Mar. 1988.
[45] Y. S. Abu-Mostafa and D. Psaltis, "Optical neural computers," *Scientific Amer.*, pp. 88–95, Mar. 1987.
[46] A. Teolis, Y. C. Pati, M. C. Peckerar, and S. Shamma, "Cascaded neural-analog networks for real time decomposition of superposed radar return signals in the presence of noise," Tech. Rep. SRC TR 89–33, Univ. of Maryland, Systems Res. Center, 1989.
[47] I. Gohberg and S. Goldberg, *Basic Operator Theory*. Boston, MA: Birkhauser, 1980.
[48] W. Rudin, *Real and Complex Analysis*. New York: McGraw-Hill, 1986.
[49] Y. C. Pati, D. Friedman, P. S. Krishnaprasad, C. T. Yao, M. Peckerar, R. Yang, and C. R. K. Marrian, "Neural networks for tactile perception," in *Proc. IEEE Int. Conf. Robotics Automat.* (Philadelphia, PA), Apr. 1988, pp. 134–139.
[50] F. Kub, I. Mack, K. Moon, C. Yao, and J. Modolo, "Programmable analog synapses for microelectronic neural networks using a hybrid digital-analog approach," in *Proc. IEEE Int. Conf. Neural Networks* (San Diego, CA), July 1988.
[51] R. Lippmann, "An introduction to computing with neural nets," *IEEE ASSP Mag.*, pp. 4–22, Apr. 1987.
[52] D. Schwartz, R. Howard, J. Denker, R. Epworth, H. Graf, W. Hubbard, L. Jackel, B. Straughn, and D. Tennant, "Dynamics of microfabricated electronic neural networks," *Appl. Phys. Lett.*, vol. 50, pp. 16–20, Apr. 1987.
[53] L. Harmon, "Touch sensing technology: A review," Tech. Rep. MSR80-03, Soc. Manufact. Engs., Dearborn, MI, 1980.

Y. C. Pati received the B.S. and M.S. degrees in electrical engineering from the University of Maryland, College Park, in 1986 and 1988, respectively. He is currently working toward the Ph.D. degree in electrical engineering at the University Maryland Systems Research Center.

His research interests include real-time processing of sensory data, control of dynamical systems, analog integrated circuits, and neural networks. He has also been with the Nanoelectronics Processing Facility of the U.S. Naval Research Laboratories, Washington, DC, since 1987 where he is an electronics engineer. His work at the Naval Research Laboratories has been in the areas of analog integrated circuit implementation of neural networks and proximity effect correction techniques for electron-beam lithography.

P. S. Krishnaprasad (S'73–M'77–SM'89–F'90) received the Ph.D. degree from Harvard University, Cambridge, MA, in 1977.

He taught at Case Western Reserve University, Cleveland, OH, from 1977 until 1980. Since 1980, he has been at the University of Maryland, College Park, where he is currently a Professor of Electrical Engineering with a joint appointment in the Systems Research Center. He has held visiting positions at the Econometric Institute at Rotterdam, the Mathematics Department of the University of California, Berkeley, the University of Groningen, and the Mathematical Sciences Institute at Cornell University, Ithaca, NY. Following his earlier work on the parametrization problem for linear systems, he has investigated a variety of problems with significant geometric content. These include nonlinear filtering problems, control of spacecraft, and more recently, the nonlinear dynamics and control of interconnected mechanical systems. His current research interests include experimental studies in the design and control of precision robotic manipulators, tactile sensing and associated inverse problems, structure-preserving numerical algorithms for Hamiltonian systems, distributed simulation environments, and many-body mechanics. He has participated in the development of the National Science Foundation sponsored Systems Research Center from its inception. He heads the Intelligent Servosystems Laboratory, a key constituent laboratory of the Center. Since 1986, he also has directed the Center of Excellence in the Control of Complex Multibody Systems sponsored by the AFOSR University Research Initiative Program.

Martin C. Peckerar (M'79–SM'89) was born in Brooklyn, NY, on June 12, 1946. He received the B.S. degree from SUNY Stony Brook in 1968, and the M.S. and Ph.D. degrees in 1971 and 1975, respectively, from the University of Maryland, College Park.

He is currently head of the Microelectronics Processing Facility at the Naval Research Laboratory, Washington, DC. His main research interest in in the application of solid-state and materials technology to problems in image processing and computation. He is the inventor of the deep-depletion CCD for X-ray and UV imaging and the laser high-brightness source for X-ray lithography. He is the coauthor (with Prof. S. P. Murarka) of the textbook *Electronic Materials and Processing* (Academic Press, 1988). He is also a part-time Professor of Electrical Engineering at the University of Maryland.